Eur. Phys. J. D **11**, 123–126 (2000)

THE EUROPEAN PHYSICAL JOURNAL D

EDP Sciences

DFT investigation of the geometrical and electronic structures of $C_{35}X$ (X = B, N and Si) clusters

Ding Changgeng[1], Yang Jinlong[1,a], Cui Xiangyuan[1], and Wang Kelin[2]

[1] Open Laboratory of Bond Selective Chemistry and Center for Fundamental Physics, University of Science and Technology of China, Hefei 230026, P.R. China
[2] Center for Fundamental Physics, University of Science and Technology of China, Hefei 230026, P.R. China

Received 8 July 1999 and Received in final form 4 October 1999

Abstract. Geometrical and electronic structures of $C_{35}X$ fullerenes with X = B, N and Si as substitutional dopants have been studied. Three non-equivalent sites in the D_{6h} structure of C_{36} have been considered for the substitution. We have found that the dopant has a strong tendency to substitute at sites where the carbon atom contributes significantly to the frontier orbitals of C_{36} and has the weakest interaction with its nearest-neighbor atoms. The relative stability of $C_{35}Si$ and $C_{35}B$ ($C_{35}N$) has been investigated and high chemical reactivity of $C_{35}Si$ has been predicted.

PACS. 71.20.Tx Fullerenes and related materials; intercalation compounds – 36.40.Cg Electronic and magnetic properties of clusters – 71.15.Mb Density functional theory, local density approximation

1 Introduction

The discovery [1] and large scale synthesis [2] of C_{60} fullerenes have stimulated much interest in the existence of similar type of clusters constructed with different species. Grossman *et al.* [3] studied recently the geometrical and electronic structures of C_{36} molecule. Shortly after this, Piskoti *et al.* [4] synthesized C_{36} crystal, and found that it is far more chemically reactive than the C_{60} structure and could easily fashion into everything from high-temperature superconductors to high-strength materials. The fact allows us to study a caged fullerene smaller than C_{60}, increasing our understanding of these novel forms of carbon. On the other hand, many physicists have worked for the interaction of the fullerene cage with foreign atoms. Several groups [5–11] produced dopant-substituted fullerenes $C_{59}X$ (X = B, N, Si, Fe, Co, Rh, and so on). Theoretically, Andreoni *et al.* [12] and Kurita *et al.* [13] studied the properties of $C_{59}B$ and $C_{59}N$ molecules. Their results showed that doping induces important changes in both ionic and electronic properties of C_{60}, and that the highest occupied molecular orbital (HOMO) is strongly localized and can act as an electron acceptor level ($C_{59}B$) or as a donor level ($C_{59}N$).

In contrast to substitutional C_{60} fullerenes, these were few studies of the doped C_{36} molecules. Kimura *et al.* and Fye *et al.* [8,9] produced experimentally silicon- and boron-doped carbon clusters including $C_{35}Si$ and $C_{35}B$. To our knowledge, except for the investigations of $C_{34}N_2$, $C_{28}N_8$, and $C_{24}N_{12}$ clusters by Grossman *et al.* [3], the theoretical study of substitutionally doped C_{36} cages has never been carried out until now.

In this paper, we performed a comprehensive first-principles study of $C_{35}X$ (X = B, N and Si), in order to explore the structural and electronic properties of these clusters. We describe our computational details in Section 2 and present our results and discussions in Section 3. Finally the conclusion is given in Section 4.

2 Computational detail

All calculations are performed using the local spin density approximation (LSDA) [14,15] provided by the DMol package [16]. Recently, excellent results for the binding energies of molecules, clusters, and solids [17–19] have been obtained by using the generalized gradient approximation (GGA), but no obvious improvement on the binding energy differences between the different fullerene structures [3]. So we do not consider the GGA corrections in the paper. We used the Vosko-Wilk-Nusair parameterization [20,21] of the local exchange-correlation energy in LSDA. The electronic structure is obtained by solving the Kohn-Sham [15] equations self-consistently. The double numerical DFT (density functional theory) atomic orbitals augmented by polarization functions are used as the variational basis set for the valence electrons while the core electrons are treated as the frozen core to save the computer effort without significantly sacrificing the accuracy. 1082 basic grid points per atom are used for the matrix integrations. Mulliken population analyses are made to obtain the charge populations on each atom. Self-consistent

[a] e-mail: jlyang@ustc.edu.cn

Table 1. The bond lengths (R_{C-C}, $R_{C-dopant}$), binding energies (E_b), HOMO, LUMO energies and HOMO-LUMO energy gaps (E_g) for C_{36} and $C_{35}X$.

	R_{C-C} (Å)	$R_{C-dopant}$ (Å)	E_b (eV)	HOMO (eV)[a]	LUMO (eV)	E_g (eV)
C_{36} (D_{6h})	1.40–1.48		293.33	0.00	0.51	0.51
$C_{35}B$ (I)	1.40–1.48	1.52, 1.52, 1.57	291.17	0.26	0.60	0.34
$C_{35}B$ (II)	1.40–1.51	1.54, 1.54, 1.56	291.65	0.19	0.84	0.65
$C_{35}B$ (III)	1.40–1.50	1.52, 1.52, 1.54	291.20	0.08	0.59	0.51
$C_{35}N$ (I)	1.40–1.48	1.39, 1.39, 1.43	290.99	0.44	0.84	0.40
$C_{35}N$ (II)	1.39–1.48	1.42, 1.42, 1.44	291.14	0.31	0.93	0.62
$C_{35}N$ (III)	1.40–1.48	1.40, 1.40, 1.41	290.50	0.41	0.82	0.41
$C_{35}Si$ (I)	1.39–1.48	1.84, 1.84, 1.91	288.47	0.07	0.53	0.46
$C_{35}Si$ (II)	1.40–1.51	1.84, 1.84, 1.88	288.79	0.02	0.44	0.42
$C_{35}Si$ (III)	1.40–1.48	1.81, 1.81, 1.81	288.28	0.08	0.55	0.47

[a] the HOMO energy level of C_{36} is given as zero.

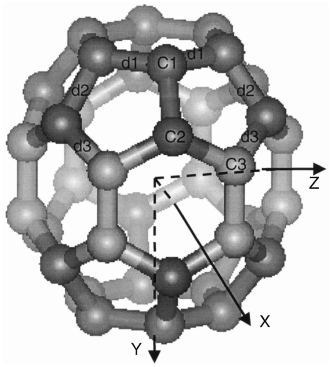

Fig. 1. Geometrical structure of the C_{36} D_{6h} cluster. C1, C2 and C3 are three non-equivalent carbon sites.

field procedure is carried out with a convergence criterion of 10^{-6} Hartree on the energy and 10^{-6} e/(Bohr)^3 on electron density. Geometry optimizations are performed using the Broyden-Fletcher-Goldfarb-Shanno (BFGS) algorithm [22] under the symmetry constraint, with a convergence criterion of 10^{-3} Hartree/Bohr on the gradient, 10^{-3} Bohr on the displacement and 10^{-5} Hartree on the energy.

3 Results and discussion

In order to make a comparison between $C_{35}X$ and pure C_{36}, we first study the pure C_{36} cluster. The electronic structures of pure C_{36} molecules have been calculated by Grossman *et al.* [3]. Their results showed the D_{6h} and D_{2d} fullerenes to be the most energetically favorable structures. We also optimized the D_{6h} and D_{2d} structures and found that the D_{6h} and D_{2d} structures are isoenergetic. However, the D_{2d} cluster, which has five groups of non-equivalent carbon sites, is too complex to study its doped fullerenes at present. So we focus our studies only on C_{36} D_{6h} cluster and its doped fullerenes in this work.

In the D_{6h} structure, C1, C2 and C3 stand for three groups of non-equivalent carbon sites, respectively. From Figure 1, we can see that C1 and C2 sites are common to two adjacent pentagons and a hexagon, whereas C3 is common to two adjacent hexagons and a pentagon. Our calculations show the following three results: (a) the HOMO and the lowest unoccupied molecular orbital (LUMO) are not degenerate, (b) the energy gap between the LUMO and HOMO is about 0.5 eV, and (c) the bond lengths are 1.40–1.48 Å, which are all in agreement with those of Grossman *et al.* [3].

When a carbon atom of C_{36} fullerene is replaced by a dopant atom, the D_{6h} symmetry is lost and the only remaining symmetry is a mirror plane. According to the symmetry of C_{36} D_{6h} structure, X atom can occupy three kinds of carbon sites: C1, C2 and C3, and they are designated as $C_{35}X$ (I), $C_{35}X$ (II) and $C_{35}X$ (III), respectively. We start the structural optimizations for $C_{35}X$ with the structure of pure C_{36}, and relax the interatomic distances by preserving the C_s symmetry. In order to check the validity of the symmetry constraint, we optimized a few structures without symmetry constraint and found that the symmetry constraint calculations give the same results as calculations with no symmetry constraints within the numerical accuracy we presented in the paper.

The main results for the structural optimization are presented in Table 1. It shows that $C_{35}X$ (II) is 0.2–0.6 eV more stable than $C_{35}X$ (I) and $C_{35}X$ (III), which can be explained from two aspects. First, we believe that chemisorption of an atom or a molecule on the fullerene, which can be regarded as a process of chemical reaction between them, is the first step in forming doped fullerene. In quantum chemistry, the frontier orbitals, the HOMO and LUMO, of reactant molecules play the leading role in their reaction. Table 2 depicts the character of the HOMO and the LUMO of C_{36}. Clearly, there is a strong contribution from C2 (7.1–7.2%/atom), which is much larger than that from C1 (0.66–0.86%/atom) and C3 (0.34–0.46%/atom). From this, we think that the external atom easily interacts with C2. Secondly, the average bond length between C2 and its nearest-neighbor (NN) atoms is larger than that between C1 (or C3) and its NN atoms, indicating the interaction between C2 and its NN atoms is the weakest. Therefore the dopant atoms prefer to substitute C2 when doping takes place.

Table 2. Orbital character of the HOMO and LUMO of the C_{36} with respect to the atomic basis. Numerals in front of C1, C2 and C3 denote numbers of atoms in each non-equivalent group.

	12C1	12C2	12C3
HOMO	10.3%	85.7%	4.1%
LUMO	7.9%	86.5%	5.5%

All the optimized geometries for the $C_{35}X$ clusters still keep the cage structure, but the regular pentagonal and hexagonal rings in C_{36} are now distorted in $C_{35}X$. The distorted values slightly depend on the relative positions of each substituted atom. We take $C_{35}Si$ as an example. The maximum atomic distortions from the C_{36} structure are 0.44 Å for $C_{35}Si$ (I), 0.42 Å for $C_{35}Si$ (II), and 0.39 Å for $C_{35}Si$ (III).

For all the $C_{35}X$ (II), the dopant atom remains three-fold coordinated, but the three bonds are not equivalent. It is interesting to compare the C–X bonds in $C_{35}X$ (II) with those observed in small molecules. For example, the B–C bond length in $B(CH_3)_3$ is 1.56 Å, the N–C bond in $N(CH_3)_3$ is 1.47 Å and the Si–C bond length in $(CH_3)_3$–Si–Si–$(CH_3)_3$ is 1.865 Å. These values are close or very close to the calculated values in substituted fullerenes. Therefore, we think that the properties of the C–X bond in $C_{35}X$ are quite similar to those in small molecules.

The main C–C bond distortions are localized on the atoms in the vicinity of the X atom. In fact, the changes of C–C bond lengths are smaller than 1% except d_2 bonds (see Fig. 1) lengthen by about 2% (for $C_{35}B$ and $C_{35}Si$) and d3 bonds shorten by about 2% (for $C_{35}N$), with respect to the corresponding bond lengths of C_{36}.

The binding energies of $C_{35}X$ (II) are a bit smaller than that of C_{36} by 0.05 eV/atom for $C_{35}B$ (II), 0.06 eV/atom for $C_{35}N$ (II) and 0.13 eV/atom for $C_{35}Si$ (II). This binding energy difference is not large, so that it is expected that $C_{35}X$ clusters would be stable. Furthermore, $C_{35}B$ (II) and $C_{35}N$ (II) is more stable than $C_{35}Si$ (II). The experiment of Kimura *et al.* [8] showed that boron atoms can be substituted in fullerenes with a much higher efficiency than silicon atoms, which is in agreement with our conclusion.

The energy levels of C_{36} and $C_{35}X$ (II) are represented in Figure 2. In Figure 2, the molecular orbitals whose energies agree with each other to within a difference of 0.05 eV are regarded as degenerate, and the length of the horizontal bar shows the orbital degeneracy. The impurity levels in $C_{35}X$ (II) are easily recognized if we compare the electronic structure of $C_{35}X$ (II) with that of C_{36}. From Table 1 and Figure 2, we can see that the energy levels near the Fermi level strongly depend on the dopant atom X for $C_{35}X$ (II). Doping with a boron atom depletes the HOMO of C_{36} by one electron and shifts it up by 0.19 eV; the energy gap between the LUMO and the HOMO is 0.65 eV. Similarly, doping with a nitrogen atom adds one electron to the LUMO. The HOMO energy is shifted down by 0.20 eV with respect to the LUMO of

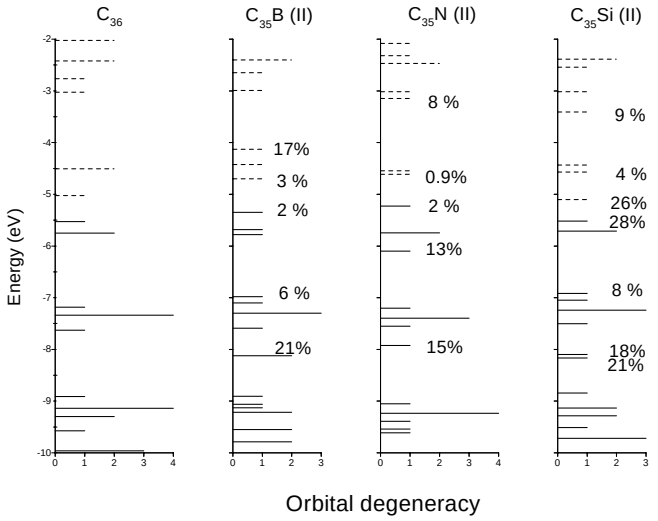

Fig. 2. Energy level diagram for C_{36}, $C_{35}B$ (II), $C_{35}N$ (II), and $C_{35}Si$ (II). Solid and dashed lines refer to occupied and unoccupied states, respectively. For $C_{35}X$ (II), the contributions of the dopant X to the character of the LUMO, HOMO and the impurity levels, given as percentage.

C_{36} and the energy gap between the LUMO and HOMO becomes 0.62 eV. For $C_{35}Si$ (II), the HOMO and LUMO levels are shifted up by 0.02 eV and down by 0.07 eV, respectively, and the LUMO-HOMO energy gap is 0.42 eV. Compared with the $C_{59}B$ and $C_{59}N$ [12], where the corresponding shifted values are 0.45 eV and 0.27 eV, respectively, we can see that the shifted effects are qualitatively the same in the two systems but smaller in $C_{35}X$ than in $C_{59}X$. In Figure 2, the contributions from the dopant atom in the LUMO, HOMO and impurity levels are labeled in terms of the percentage of population. The dopant atom contributions in the LUMO and HOMO are very small for $C_{35}B$ (II) and $C_{35}N$ (II), whereas those in the LUMO and HOMO are very strong for $C_{35}Si$ (II). This indicates that $C_{35}Si$ (II) is very reactive at the Si site. We can expect that the $C_{35}Si$ (II) cluster is promising in the formation of new compounds.

Finally, we have also calculated the dipole moments of the $C_{35}X$ (II) (see Tab. 3). The dipole moment is oriented inwards for the $C_{35}B$ (II), while the dipole moments are oriented outwards for the $C_{35}N$ (II) and the $C_{35}Si$ (II). However, the orientations of dipole moments are not exactly radial, which is different from the $C_{59}X$ [12]. This difference is due to the fact that the C_{60} molecule is more nearly spherical than the C_{36} molecule. The magnitudes of dipole moment of $C_{35}B$ (II), $C_{35}N$ (II) and $C_{35}Si$ (II) are about 0.23 Debye, 0.47 Debye and 0.27 Debye, respectively. Table 4 lists the Mulliken populations of C1, X and C3 in the $C_{35}X$ (II). With reference to the Mulliken population in the C_{36}, one can easily see how the s and p electron count decreases for C1 and C3 in the $C_{35}N$ (II), whereas the s, p electron count increases for C1 and C3 in the $C_{35}B$ (II) and $C_{35}Si$ (II). We observe a net charge transfer to the dopant site of 0.01 e for the $C_{35}B$ (II), 0.30 e for the $C_{35}N$ (II), and 0.07 e for the $C_{35}Si$ (II).

Table 3. The dipole moments (Debye) of the $C_{35}X$ (II).

	x-component	y-component	z-component	magnitude
$C_{35}B$ (II)	−0.23	0.01	0.00	0.23
$C_{35}N$ (II)	0.39	−0.26	0.00	0.47
$C_{35}Si$ (II)	0.26	0.05	0.00	0.27

Table 4. The Mulliken valence charge populations of dopant atom and its nearest-neighbor carbon atoms in the C_{36} and $C_{35}X$ (II).

		C_{36}	$C_{35}B$ (II)	$C_{35}N$ (II)	$C_{35}Si$ (II)
	s	1.23	1.26	1.19	1.32
C1	p	2.61	2.73	2.49	2.72
	d	0.17	0.14	0.20	0.13
	net charge	−0.01	−0.13	0.12	−0.17
	s	1.25	1.09	1.42	1.31
X^a	p	2.61	1.78	3.69	2.33
	d	0.18	0.15	0.19	0.43
	net charge	−0.03	−0.01	−0.30	−0.07
	s	1.24	1.27	1.21	1.33
C3	p	2.54	2.70	2.38	2.66
	d	0.18	0.14	0.21	0.14
	net charge	0.04	−0.12	0.20	−0.13

[a] X stands for C2 in pure C_{36} cluster.

The magnitudes of these charge transfers correlate with that of the dipole moments.

4 Conclusion

In conclusion, we have reported a comprehensive study of the geometrical and electronic structures of dopant-substituted fullerenes $C_{35}X$ (X = B, N and Si) using the first-principles LSDA method. All the optimized geometries for the $C_{35}X$ clusters still keep the cage structures, but the regular pentagonal and hexagonal rings in C_{36} are now distorted in $C_{35}X$. The deformation of the fullerene network due to the substituted dopant atom slightly depends on the relative positions of each substituted atom. Moreover, $C_{35}X$ (II) clusters are more stable than the corresponding $C_{35}X$ (I) and $C_{35}X$ (III) clusters. These results show that the X atom has a strong tendency to substitute the site where the substituted carbon atom has a significant contribution for the frontier orbitals of C_{36} and that has the weakest interaction with its nearest-neighbor atoms. From the viewpoint of binding energy, we have found that the $C_{35}B$ and $C_{35}N$ are more stable than $C_{35}Si$, which is consistent with the experiment of Kimura *et al.*

The electronic structure of $C_{35}X$ (II) varies with the dopant atom X. The energy gap (E_g) between the LUMO and HOMO is 0.65 for $C_{35}B$ (II), 0.62 for $C_{35}N$ (II), and 0.42 eV for $C_{35}Si$ (II). The contributions from the dopant atom in the LUMO and HOMO are very strong for $C_{35}Si$ (II), indicating $C_{35}Si$ (II) has high chemical reactivity.

This work was partially supported by the National "Climb" Project of China, by the National "863" Project of China, by the National Natural Science Foundation of China, and by the Foundation of the Chinese Academy of Science. The HPCC, NSC and SC&CG laboratory of USTC are acknowledged for providing us powerful computational service.

References

1. H.W. Kroto, J.R. Heath, S.S. O'Brien, R.F. Curl, R.E. Smalley, Nature **162**, 318 (1985).
2. W. Krätschmer, L.D. Lamb, K. Fostiropoulos, D.R. Huffiman, Nature **347**, 354 (1990).
3. J.C. Grossman, M. Côté, S.G. Louie, M.L. Cohen, Chem. Phys. Lett. **284**, 344 (1998).
4. C. Piskoti, J. Yarger, A. Zettl, Nature **393**, 771 (1998).
5. T. Guo, C. Jin, R.E. Smalley, J. Phys. Chem. **95**, 4948 (1991).
6. R. Yu, M. Zhan, D. Cheng, S. Yang, Z. Liu, L. Zheng, J. Phys. Chem. **99**, 1818 (1995).
7. J.C. Hummelen, B. Knight, J. Pavlovich, R. Gonzàlez, F. Wudl, Science **269**, 1554 (1995).
8. T. Kimura, T. Sugai, H. Shinohara, Chem. Phys. Lett. **256**, 269 (1996).
9. J.L. Fye, M.F. Jarrold, J. Phys. Chem. A **101**, 1836 (1997).
10. W. Branz, I.M.L. Billas, N. Malinowski, F. Tast, M. Heinebrodt, T.P. Martin, J. Chem. Phys. **109**, 3425 (1998).
11. C. Ray, M. Pellarin, J.L. Lermé, J.L. Vialle, M. Broyer, X. Blase, P. Mélinon, P. Kéghélian, A. Perez, Phys. Rev. Lett. **80**, 5365 (1998).
12. W. Andreoni, F. Gygi, M. Parinello, Chem. Phys. Lett. **190**, 159 (1992).
13. N. Kurita, K. Kobayashi, H. Kumahora, K. Tago, K. Ozawa, Chem. Phys. Lett. **198**, 95 (1992).
14. P. Hohenberg, W. Kohn, Phys. Rev. **136**, B864 (1964).
15. W. Kohn, L.J. Sham, Phys. Rev. **140**, A1133 (1965).
16. Dmol v960, Biosym Technologies, San Diego CA, 1996.
17. V. Ozoliηs̃, M. Körling , Phys. Rev. B **48**, 18304 (1993).
18. H. Groñbeck, A. Rosén, J. Chem. Phys. **107**, 10620 (1997).
19. C. Ding, J. Yang, Q. Li, K. Wang, F. Toigo, Phys. Lett. A **256**, 417 (1999).
20. S.H. Vosko, L. Wilk, M. Nusair, Can. J. Phys. **58**, 1200 (1980).
21. D.M. Ceperley, B.J. Alder, Phys. Rev. Lett. **45**, 556 (1980).
22. R. Fletcher, *Practical methods of optimization* (Wiley, New York, 1980), Vol. 1.